

Partially Coherent Double-Phase Holography in Visible Wavelength Using Meta-Optics

Saswata Mukherjee,* Quentin A. A. Tanguy, Johannes E. Fröch, Aamod Shanker, Karl F. Böhlinger, Steven Brunton, and Arka Majumdar*



Cite This: <https://doi.org/10.1021/acsp Photonics.2c02016>



Read Online

ACCESS |



Metrics & More



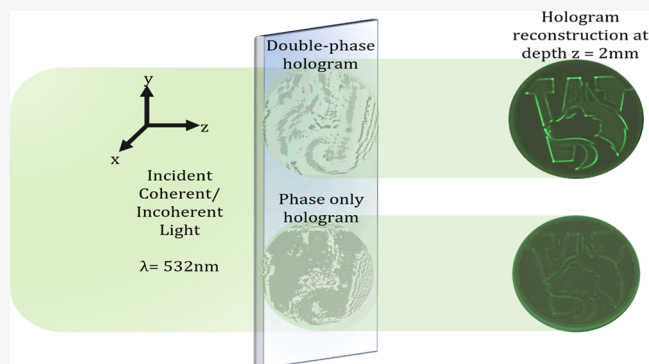
Article Recommendations



Supporting Information

ABSTRACT: Ultrathin flat meta-optics have shown great promise for holography in recent years. However, most of the reported meta-optical holograms rely on only phase modulation and neglect the amplitude information. Modulation of both amplitude and phase in meta-optics requires either polarization-sensitive meta-atoms or complex scatterers with stringent fabrication requirements. Additionally, almost all of the meta-optical holograms were measured under laser illumination. Here, we adopt the concept of double-phase holography, to report polarization-independent holography with both amplitude and phase modulation, using dielectric meta-optics. We validate the implementation of complex phase hologram by measuring an improvement of structural similarity of the reconstructed hologram by nearly 3 times over phase-only holograms. Finally, we demonstrate that meta-optical holography can also be realized using partially incoherent light from a light-emitting diode. This observation can significantly reduce the alignment complexity and speckles in laser-based meta-optical holography.

KEYWORDS: diffractive optics, meta-optics, digital holography, double-phase encoding



making CGHs primarily limited to either phase-only or amplitude-only modulation. This typically results in a poor signal-to-noise ratio (SNR) of the reconstructed image. A solution to this problem is achieved by implementing both amplitude and phase modulation via dual-phase holography,^{5–7} where each value of the complex phase is coded using two different pixels. While dual-phase holography improves the SNR, it comes at the cost of reduced spatial resolution.⁸

INTRODUCTION

Holography is a key concept for next-generation display technologies, widely being explored for three-dimensional (3D) displays and near-eye visors for augmented and virtual reality, where an immersive visual experience for the user is of utmost importance. The fundamental principle of holography relies on the reconstruction of the light field produced by a screen containing both amplitude and phase information.¹ The simplest configuration to store and recreate a hologram is achieved by recording the interference patterns formed by light scattered by an object and a reference coherent beam.¹ While this technique creates crisp scenes, the requirement of recording a real object and a spatially and temporally coherent light source severely restricts applications, as typically only existing and static scenes are recordable. These particular limitations were resolved with the advent of digital computers and the emergence of spatial light modulators (SLM), which brought forth the development of computer-generated holography (CGH).^{2,3} In CGH, the phase profile for any desired image is generated via computational algorithms, and subsequently the phase profile is displayed on an SLM, which under coherent light illumination creates the image at the desired plane. Based on the same principle, static holograms can be implemented using patterned surfaces, such as diffractive optics.⁴ However, traditional SLMs or diffractive optics cannot modulate both amplitude and phase,

making CGHs primarily limited to either phase-only or amplitude-only modulation. This typically results in a poor signal-to-noise ratio (SNR) of the reconstructed image. A solution to this problem is achieved by implementing both amplitude and phase modulation via dual-phase holography,^{5–7} where each value of the complex phase is coded using two different pixels. While dual-phase holography improves the SNR, it comes at the cost of reduced spatial resolution.⁸

In recent years, meta-optics has emerged as a promising alternative to implement a desired phase profile. Meta-optics are artificially manufactured arrays of subwavelength scatterers,^{9,10} which shape the optical wavefront with high spatial resolution. A distinct advantage is that the subwavelength pitch of scatterers precludes any higher-order diffraction, thus maximizing light in the zeroth-order diffraction and making it more efficient than traditional diffractive optics.^{11,12} These properties have inspired many researchers to demonstrate holography with meta-optics.^{13–21} However, for the majority of these works, phase-

Received: December 28, 2022

only modulation has been considered. To implement complex phase holography, i.e., both phase and amplitude modulation, meta-atoms with complex orientations and shapes were utilized in THz domain,^{22,23} but their fabrication will be difficult in the visible wavelength. The other approaches are generally polarization-sensitive.^{24,25} Complex phase modulation can also be achieved using multilayer meta-optics,^{26,27} where the first meta-optic modulates the amplitude and a subsequent one modulates the phase of the transmitted light. However, such bilayer meta-optics are arduous to fabricate due to their requirement of precise alignments. Additionally, one needs to rely on high-contrast materials like silicon or metal as they need to be embedded in polymers. This presents a limitation for low-index materials like silicon nitride²⁸ or titanium dioxide,²⁹ which are transparent in the visible wavelength.

In this work, we report polarization-independent complex phase modulated holography using a single visible meta-optics containing simple square pillar meta-atoms. We employ double-phase holography to implement the complex phase modulation. We note that several other works have previously focused on improving the double-phase holography,^{30,31} for instance, through improving the algorithms to generate the hologram or by imposing other limits to improve reconstructions, our contribution in this work is to implement double-phase holography using meta-optics. Thanks to the subwavelength pitch in a meta-optic, we can achieve a very high space-bandwidth product, and thus the main limitation of double-phase holography is not as severe as in a meta-optic. We establish the efficacy of double-phase holography by demonstrating a higher structural similarity index metric (SSIM) of double-phase holograms over phase-only holograms, under both coherent and incoherent green illumination. The ability to create meta-optical holograms using incoherent illumination from light-emitting diodes can significantly simplify the optical arrangement, making them more applicable for practical applications, including near-eye displays for augmented and virtual reality.³² Additionally, the ability to coherently manipulate the optical field will be important for free-space vector-matrix multiplication and optical computing.³³

METHODOLOGY

Figure 1 shows the schematic where the meta-optical hologram is irradiated with a coherent or incoherent light source ($\lambda = 532$ nm), and the images are reconstructed at the imaging plane $z = 2$ mm away from the meta-optic. The meta-optics is polarization-independent and designed to generate the images at the desired wavelength. Here, we used two objects, “digit W and Husky”, and a part of the United States Air Force (USAF) test targets. We assumed the object to be virtually located at the imaging plane ($z = 2$ mm) from the meta-optics and used the angular spectrum method³⁴ to estimate the desired complex phase of the meta-optic. We applied the double-phase encoding technique to generate the complex field in the meta-hologram. We also extracted the real part of the phase from the complex electric field to realize a phase-only meta-optic hologram. Additionally, another phase-only meta-optic hologram was realized using the Gerchberg–Saxton algorithm,³⁵ having imaging plane and size identical to other holograms.

The procedure for realizing the double-phase hologram is shown in Figure 2. Let us assume the target complex hologram U_F can be expressed as $U_F(x, y) = A_1(x, y) \cdot e^{i\varphi(x, y)}$, where $\varphi(x, y)$ is the phase and $A_1(x, y)$ is normalized amplitude with values in the range between 0 and 2. We can then rewrite $A_1(x, y) = e^{i\theta(x, y)} +$

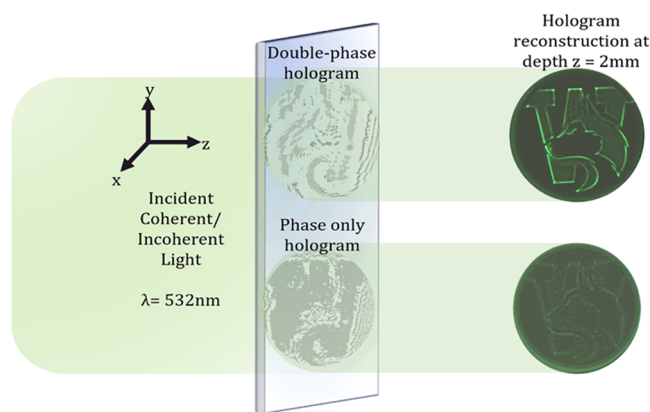


Figure 1. Illustration of holography using a double-phase hologram and a phase-only hologram realized by all-dielectric meta-optics. Under incident green light (both coherent and incoherent), the device displays an image at the desired plane. The image quality with double-phase holography is expected to be better than simple phase-only hologram.

$e^{-i\theta(x, y)} = 2 \cos \theta(x, y)$, where $\theta(x, y) \in [-\pi, \pi]$. Hence, we can rewrite U_F as

$$U_F(x, y) = h_1(x, y) \times M_1 + h_2(x, y) \times M_2$$

with $h_1 = e^{i[\varphi(x, y) + \theta(x, y)]}$ and $h_2 = e^{i[\varphi(x, y) - \theta(x, y)]}$. Thus, at each point (x, y) , we obtain two-phase values: $\varphi(x, y) \pm \theta(x, y)$. The complementary binary masks (M_1 and M_2)³⁶ with two-dimensional (2D) checkerboard patterns, help reduce the required phase at each point to a single value.

This sampling technique is similar to the random mask encoding for multiplexing phase-only filters,³⁷ except we select two complementary binary functions under Nyquist limit. This phase profile can then be translated into a meta-optic and upon illumination with light, a hologram forms at the desired plane, as schematically depicted in Figure 1.

DESIGN

The meta-optical hologram consists of an array (periodicity $p = 350$ nm) of meta-atoms, here subwavelength silicon nitride square pillars with height $t = 560$ nm on quartz substrate (Figure 3a). We keep a blanket 40 nm thick silicon nitride film on the quartz substrate to ensure mechanical stability. We found the effect of the blanket thin Si_3N_4 film to be negligible as detailed in the Supporting Materials. The width w of the pillars was varied between 75 and 330 nm to cover the entire 2π phase modulation at a wavelength of $\lambda = 530$ nm with near-unity transmission (Figure 3b), as simulated using rigorous coupled-wave analysis (RCWA).³⁸ These meta-atoms also ensure a moderate aspect ratio and can be easily fabricated. To design the meta-optics, we selected 12 different scatterers (all with transmission greater than 80%), i.e., the resulting hologram has 12 discrete phase levels. Figure 3c shows the scanning electron microscope images of the fabricated meta-optic (details in the Materials and Methods Section).

RESULTS

The efficacy of the double-phase holograms over the phase-only holograms was then experimentally assessed. Either a laser or a light-emitting diode is used to illuminate the meta-holograms (Figure 4a), and the reconstructed image was captured using a movable microscope (details in the Materials and Methods Section).

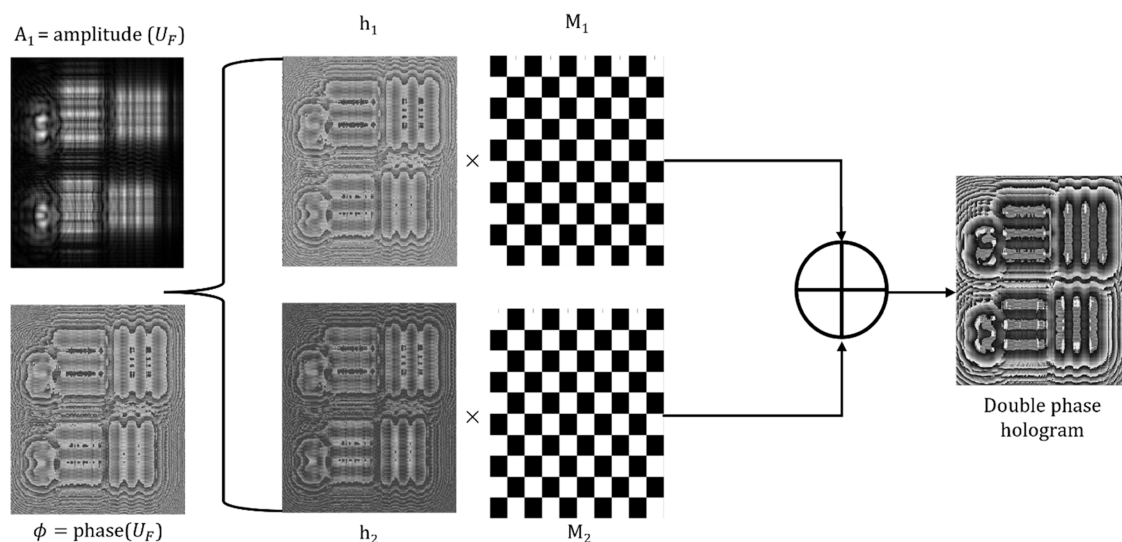


Figure 2. Flowchart of double-phase encoding method for complex field modulation. First, the complex hologram U_F is calculated from the desired ground truth. Then, the amplitude and phase from the complex field are extracted for the decomposition of the given complex field into two pure phase functions h_1 and h_2 using the phase encoding technique.⁵ Two complementary 2D binary masks (checkerboard patterns) are superimposed on the two pure phase elements to reduce it to one phase value at every coordinate (x,y) .

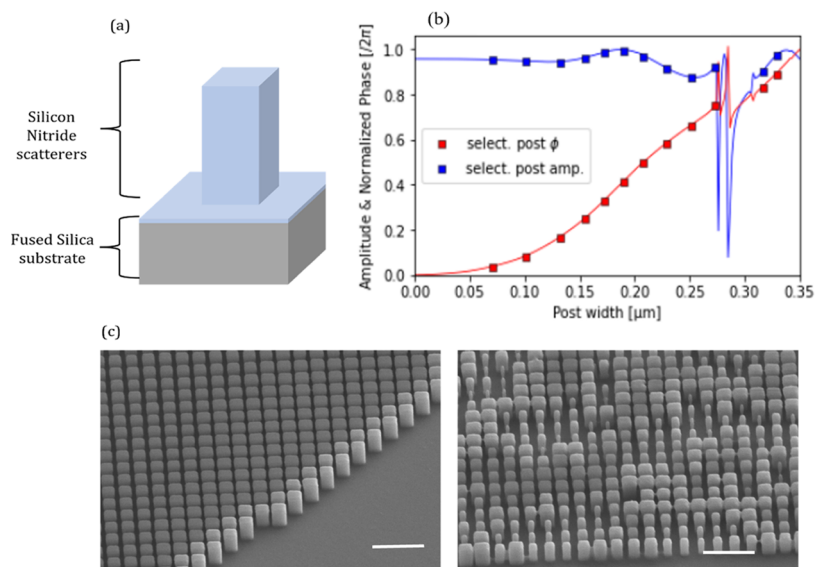


Figure 3. (a) Schematic of silicon nitride pillars with width w , pitch p , and height t . (b) Transmission amplitude and phase of the nano-pillars as a function of pillar width, simulated using RCWA.³⁸ (c) Scanning electron microscope (SEM) images of part of the meta-optical hologram showing the nano-pillars. Scale bar: 1 μm .

Using two different ground truth images (Figure 4b), we first compare the performance of the holography for three cases under coherent green illumination: complex-valued phase with double-phase holography (see the Methodology Section), phase-only hologram with only real part of the complex-valued phase, and phase hologram designed via Gerchberg–Saxton (GS) algorithm. The comparison to the phase-only hologram with only real part of the complex-valued phase allows us to assess the efficacy of the double-phase holograms implementing the full complex phase. The comparison with iterative GS holograms is reported to show that a single-step calculation can create a hologram comparable to that of an iterative process, thanks to the ability to code the whole complex phase. A low-pass filter was applied to the target image to blur the boundaries of the object so that the outer edges of the hologram have low amplitudes

(Section S1). This correctly modulates the higher spatial frequencies in the hologram and removes the unwanted edge enhancements (see the Supporting Information). Both in the simulation (Figure 4c) and experiment (Figure 4d), the double-phase holography shows better reconstruction results compared to phase-only holography and comparable results to GS holograms. However, the GS holograms have the problems of unwanted speckles in reconstruction due to destructive interference occurring within the target image region. To quantitatively validate our claim, we calculated the structural similarity metrics (SSIM) between the reconstructed images and the ground truth in the region of interest containing only the image (Table 1). We clearly observe superior performance of the double-phase holography.

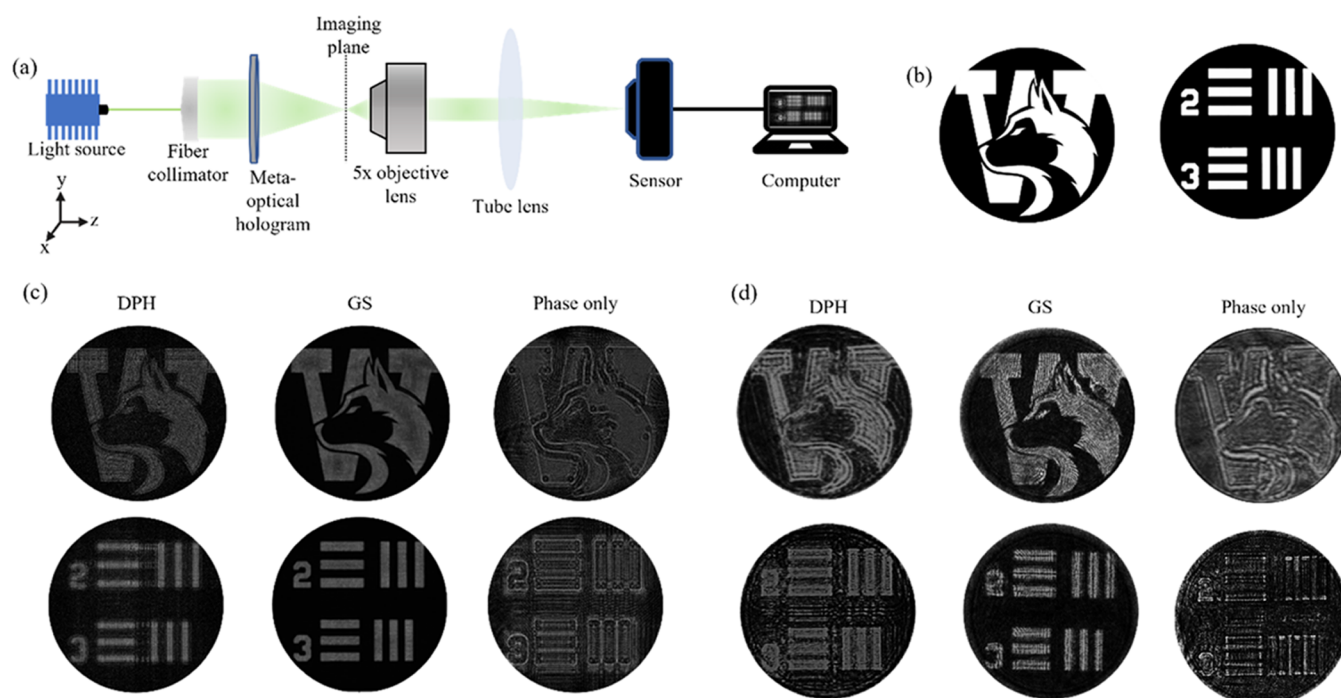


Figure 4. (a) Schematic of optical setup to test the meta-optical holography. (b) Appropriately cropped original object patterns of “W and Husky” and “USAF target portion” are the ground truth image. (c) Simulated and (d) experimentally measured holographic reconstruction for three methods: double-phase holography (DPH), Gerchberg–Saxton holography (GS), and amplitude-discarded phase-only holography.

Table 1. Structural Similarity Metrics of Different Types of Measured Holograms for Two Different Objects Using Both Coherent and Incoherent Illumination

	DPH		GS		phase-only	
	coherent	incoherent	coherent	incoherent	coherent	incoherent
USAF target portion	0.5834	0.5703	0.6408	0.5144	0.2621	0.2185
W and Husky	0.5855	0.5496	0.5728	0.5251	0.2736	0.2301

Although for holography, coherent illumination typically yields better results, incoherent light sources such as light-emitting diodes can be significantly more cost-effective. Additionally, the speckle under incoherent illumination is minimal, whereas under laser illumination, we often need to rely on extra optics to reduce spectral coherence. Hence, we tested the meta-optical holograms under incoherent illumination. Here, we use a green light-emitting diode (Thorlabs M530F1) at a central wavelength of 525 nm and linewidth ~ 20 nm. The resulting holograms are shown in Figure 5. While coherent illumination does provide better holographic reconstruction, we demonstrate that a comparable quality for reconstruction can be achieved using incoherent illumination, as can be seen in the SSIMs in Table 1. Furthermore, we observed that the double-phase holograms achieved higher SSIM even under incoherent illumination compared to the amplitude-discarded phase-only approach under coherent illumination. This is further confirmed by peak signal-to-noise ratio analysis for the different holograms, as shown in Supporting Section S2. We emphasize that this is the first-time incoherent holography has been reported using meta-optics, which can potentially enable a drastic reduction of the form factor of near-eye visors.³⁹

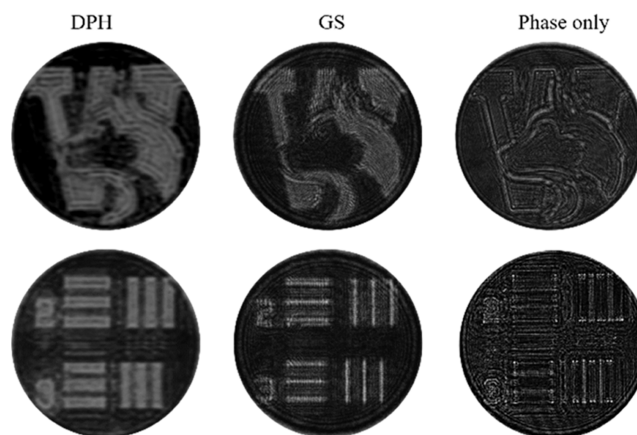


Figure 5. Hologram reconstruction with incoherent illumination using green light-emitting diodes with a bandwidth of ~ 20 nm. DPH—double-phase hologram; GS—Gerchberg–Saxton hologram; phase-only holograms.

CONCLUSIONS

We have demonstrated complex field-modulated holography in meta-optics using a double-phase encoding technique. Our proposed approach is polarization-independent and does not rely on complicated meta-atoms. Moreover, we demonstrated

meta-optical holography under an incoherent light-emitting diode source. While partially incoherent holography has been reported in CGH literature in the past, this is the first time it is demonstrated in a meta-optic. We compared three meta-hologram types (complex phase, amplitude-discarded phase-only, and phase-only via GS algorithm) using SSIM and demonstrated the superiority of double-phase hologram. This work offers a robust and generalizable method for realizing the primary promise of meta-optics: to modulate complex fields at will. Such ability to modulate complex fields will be beneficial for other applications, including free-space optical computing.

MATERIALS AND METHODS

Fabrication Process. We fabricated the meta-optical holograms using a 500-micron-thick fused silica wafer and depositing 600 nm of silicon nitride using plasma-enhanced chemical vapor deposition at 350 °C. A 300 nm thick layer of ZEP 520A followed by a thin film of anticharge polymer (DisCharge H₂O) was spin-coated on top of Si₃N₄ thin film. Next, the hologram patterns are written by electron beam lithography (JEOL 6300) at a beam voltage of 100 kV, beam current of 8000 pA, and a base dose of 275 μC/cm² and appropriate proximity effect corrections. The resulting designs are developed in a solution of amyl acetate and cleaned with isopropyl alcohol. The exposed and developed samples are then placed in a physical evaporator to deposit roughly 60 nm of aluminum oxide. The dissolution of the remaining resist performs lift-off in *N*-methyl-2-pyrrolidone (NMP) at 90 °C for 12 h. Finally, the pattern is transferred from the aluminum oxide mask to the Si₃N₄ by using a fluorine-based RIE process (Oxford) leaving a total thickness of 10 nm of alumina over 560 nm of Si₃N₄.

Optical Characterization. A set of collimating optics passes coherent light (Laserglow; wavelength: 532 nm; max power: 150 mW) to the meta-optics. Light is collected and analyzed using a movable microscope. An infinity-corrected 5× objective (Nikon Plan Fluor 5×, 0.15 NA) collects light scattered by the meta-optic at 2 mm away from the optic and passes it through a tube lens (Thorlabs, *f* = 200 mm). Then, an iris is used to cut off unwanted light from reaching the CMOS sensor (Point Grey CMLN 13S2M CS). The same experiment was repeated with incoherent light by replacing the green laser with the green light-emitting diode (Thorlabs M530F1) while keeping the rest of the setup intact.

ASSOCIATED CONTENT

Supporting Information

The Supporting Information is available free of charge at <https://pubs.acs.org/doi/10.1021/acsp Photonics.2c02016>.

Effect of blurring the image on reconstruction; quality of the reconstructed holograms discussed using PSNR as a figure of merit; and graphical analysis of the effect of blanket layer thickness on the phase profile (PDF)

AUTHOR INFORMATION

Corresponding Authors

Saswata Mukherjee – Department of Electrical and Computer Engineering, University of Washington, Seattle, Washington 98195, United States; orcid.org/0000-0001-6719-8785; Email: saswata7@gmail.com

Arka Majumdar – Department of Electrical and Computer Engineering, University of Washington, Seattle, Washington

98195, United States; Department of Physics, University of Washington, Seattle, Washington 98195, United States; orcid.org/0000-0003-0917-590X; Email: arka@uw.edu

Authors

Quentin A. A. Tanguy – Department of Electrical and Computer Engineering, University of Washington, Seattle, Washington 98195, United States

Johannes E. Frösch – Department of Electrical and Computer Engineering, University of Washington, Seattle, Washington 98195, United States

Aamod Shanker – Department of Electrical and Computer Engineering, University of Washington, Seattle, Washington 98195, United States

Karl F. Böhringer – Department of Electrical and Computer Engineering, University of Washington, Seattle, Washington 98195, United States; Institute for Nano-Engineered Systems, University of Washington, Seattle, Washington 98195, United States; orcid.org/0000-0002-9428-2648

Steven Brunton – Department of Mechanical Engineering, University of Washington, Seattle, Washington 98195, United States

Complete contact information is available at: <https://pubs.acs.org/10.1021/acsp Photonics.2c02016>

Notes

The authors declare no competing financial interest.

ACKNOWLEDGMENTS

The research was supported by NSF- 2040527. Part of this work was conducted at the Washington Nanofabrication Facility/Molecular Analysis Facility, a National Nanotechnology Coordinated Infrastructure (NNCI) site at the University of Washington with partial support from the National Science Foundation via awards NNCI-1542101 and NNCI-2025489.

REFERENCES

- (1) Leith, E. N.; Upatnieks, J. Reconstructed Wavefronts and Communication Theory*. *J. Opt. Soc. Am.* **1962**, *52*, No. 1123.
- (2) Yu, H.; Lee, K.; Park, J.; Park, Y. Ultrahigh-Definition Dynamic 3D Holographic Display by Active Control of Volume Speckle Fields. *Nat. Photonics* **2017**, *11*, 186–192.
- (3) Slinger, C.; Cameron, C.; Stanley, M. Computer-Generated Holography as a Generic Display Technology. *Computer* **2005**, *38*, 46–53.
- (4) Betin, A. Y.; Dontchenko, S. S.; Kovalev, M. S.; Odinkov, S. B.; Solomashenko, A. B.; Zlokazov, E. Y. In *A Combination of Computer-Generated Fourier Holograms and Light Guide Substrate with Diffractive Optical Elements for Optical Display and Sighting System*, Digital Holography and Three-Dimensional Imaging, DH 2015; Optica Publishing Group, 2015.
- (5) Hsueh, C. K.; Sawchuk, A. A. Computer-Generated Double-Phase Holograms. *Appl. Opt.* **1978**, *17*, No. 3874.
- (6) Arrizón, V.; Sánchez-de-la-Llave, D. Double-Phase Holograms Implemented with Phase-Only Spatial Light Modulators: Performance Evaluation and Improvement. *Appl. Opt.* **2002**, *41*, No. 3436.
- (7) Maimone, A.; Georgiou, A.; Kollin, J. S. Holographic Near-Eye Displays for Virtual and Augmented Reality. *ACM Trans. Graphics* **2017**, *36*, 1–16.
- (8) Chakravarthula, P.; Peng, Y.; Kollin, J.; Fuchs, H.; Heide, F. Wirtinger Holography for Near-Eye Displays. *ACM Trans. Graphics* **2019**, *38*, 1–13.
- (9) Yu, N.; Genevet, P.; Kats, M. A.; Aieta, F.; Tetienne, J.-P.; Capasso, F.; Gaburro, Z. Light Propagation with Phase Discontinuities:

Generalized Laws of Reflection and Refraction. *Science* **2011**, *334*, 333–337.

(10) Zhan, A.; Colburn, S.; Trivedi, R.; Fryett, T. K.; Dodson, C. M.; Majumdar, A. Low-Contrast Dielectric Metasurface Optics. *ACS Photonics* **2016**, *3*, 209–214.

(11) Meinzer, N.; Barnes, W. L.; Hooper, I. R. Plasmonic Meta-Atoms and Metasurfaces. *Nat. Photonics* **2014**, *8*, 889–898.

(12) Yu, N.; Capasso, F. Flat Optics with Designer Metasurfaces. *Nat. Mater.* **2014**, *13*, 139–150.

(13) Hu, Y.; Luo, X.; Chen, Y.; Liu, Q.; Li, X.; Wang, Y.; Liu, N.; Duan, H. 3D-Integrated Metasurfaces for Full-Colour Holography. *Light Sci. Appl.* **2019**, *8*, No. 86.

(14) Huang, L.; Zhang, S.; Zentgraf, T. Metasurface Holography: From Fundamentals to Applications. *Nanophotonics* **2018**, *7*, 1169–1190.

(15) Zheng, G.; Mühlenbernd, H.; Kenney, M.; Li, G.; Zentgraf, T.; Zhang, S. Metasurface Holograms Reaching 80% Efficiency. *Nat. Nanotechnol.* **2015**, *308*–312.

(16) Yoon, G.; Lee, D.; Nam, K. T.; Rho, J. Pragmatic Metasurface Hologram at Visible Wavelength: The Balance between Diffraction Efficiency and Fabrication Compatibility. *ACS Photonics* **2018**, *5*, 1643–1647.

(17) Wang, L.; Kruk, S.; Tang, H.; Li, T.; Kravchenko, I.; Neshev, D. N.; Kivshar, Y. S. Grayscale Transparent Metasurface Holograms. *Optica* **2016**, *3*, No. 1504.

(18) Ni, X.; Kildishev, A.; Shalaev, V. M. Metasurface Holograms for Visible Light. *Nat. Commun.* **2013**, *4*, No. 2807.

(19) Kim, J.; Yang, Y.; Badloe, T.; Kim, I.; Yoon, G.; Rho, J. Geometric and Physical Configurations of Meta-Atoms for Advanced Metasurface Holography. *InfoMat* **2021**, *3*, 739–754.

(20) Kim, J.; Seong, J.; Yang, Y.; Moon, S. W.; Badloe, T.; Rho, J. Tunable Metasurfaces towards Versatile Metalenses and Metaholograms: A Review. *Adv. Photonics* **2022**, *4*, No. 024001.

(21) Kim, J.; Jeon, D.; Seong, J.; Badloe, T.; Jeon, N.; Kim, G.; Kim, J.; Baek, S.; Lee, J. L.; Rho, J. Photonic Encryption Platform via Dual-Band Vectorial Metaholograms in the Ultraviolet and Visible. *ACS Nano* **2022**, *16*, 3546–3553.

(22) Zhang, X.; Wang, Q.; Xu, Q.; Zhang, X.; Tian, C.; Xu, Y.; Gu, J.; Tian, Z.; Ouyang, C.; Han, J.; Zhang, W. All-Dielectric Meta-Holograms with Holographic Images Transforming Longitudinally. *ACS Photonics* **2018**, *5*, 599–606.

(23) Wang, Q.; Zhang, X.; Xu, Y.; Gu, J.; Li, Y.; Tian, Z.; Singh, R.; Zhang, S.; Han, J.; Zhang, W. Broadband Metasurface Holograms: Toward Complete Phase and Amplitude Engineering. *Sci. Rep.* **2016**, *6*, No. 32867.

(24) Overvig, A. C.; Shrestha, S.; Malek, S. C.; Lu, M.; Stein, A.; Zheng, C.; Yu, N. Dielectric Metasurfaces for Complete and Independent Control of the Optical Amplitude and Phase. *Light Sci. Appl.* **2019**, *8*, No. 92.

(25) Lee, G. Y.; Yoon, G.; Lee, S. Y.; Yun, H.; Cho, J.; Lee, K.; Kim, H.; Rho, J.; Lee, B. Complete Amplitude and Phase Control of Light Using Broadband Holographic Metasurfaces. *Nanoscale* **2018**, *10*, 4237–4245.

(26) Zhou, Y.; Kravchenko, I. I.; Wang, H.; Zheng, H.; Gu, G.; Valentine, J. Multifunctional Metaoptics Based on Bilayer Metasurfaces. *Light Sci. Appl.* **2019**, *8*, No. 80.

(27) Tanaka, K.; Arslan, D.; Fasold, S.; Steinert, M.; Sautter, J.; Falkner, M.; Pertsch, T.; Decker, M.; Staude, I. Chiral Bilayer All-Dielectric Metasurfaces. *ACS Nano* **2020**, *14*, 15926–15935.

(28) Colburn, S.; Zhan, A.; Bayati, E.; Whitehead, J.; Ryou, A.; Huang, L.; Majumdar, A. Broadband Transparent and CMOS-Compatible Flat Optics with Silicon Nitride Metasurfaces [Invited]. *Opt. Mater. Express* **2018**, *8*, No. 2330.

(29) Khorasaninejad, M.; Chen, W. T.; Devlin, R. C.; Oh, J.; Zhu, A. Y.; Capasso, F. Metalenses at Visible Wavelengths: Diffraction-Limited Focusing and Subwavelength Resolution Imaging. *Science* **2016**, *352*, 1190–1194.

(30) Sui, X.; He, Z.; Jin, G.; Chu, D.; Cao, L. Band-Limited Double-Phase Method for Enhancing Image Sharpness in Complex Modulated Computer-Generated Holograms. *Opt. Express* **2021**, *29*, 2597–2612.

(31) Zhang, J.; Zhang, Z.; Li, H.; Liu, X. Optimizing Double-Phase Method Based on Gradient Descent Algorithm with Complex Spectrum Loss Function. *Opt. Commun.* **2022**, *514*, No. 128136.

(32) Xiong, J.; Hsiang, E. L.; He, Z.; Zhan, T.; Wu, S. T. Augmented Reality and Virtual Reality Displays: Emerging Technologies and Future Perspectives. *Light Sci. Appl.* **2021**, *10*, No. 216.

(33) Ryou, A.; Whitehead, J.; Zhelyeznyakov, M.; Anderson, P.; Keskin, C.; Bajcsy, M.; Majumdar, A. Free-Space Optical Neural Network Based on Thermal Atomic Nonlinearity. *Photonics Res.* **2021**, *9*, B128–B134.

(34) Goodman, J. W. *Introduction to Fourier Optics*, 3rd ed.; Roberts & Company Publishers: Englewood, Colorado, USA, 2005.

(35) Gerchberg, R. W.; Saxton, W. O. Practical algorithm for the determination of phase from image and diffraction plane pictures. *Optik* **1972**, *35*, 237–246.

(36) Mendoza-Yero, O.; Mínguez-Vega, G.; Lancis, J. Encoding Complex Fields by Using a Phase-Only Optical Element. *Opt. Lett.* **2014**, *39*, No. 1740.

(37) Davis, J. A.; Cottrell, D. M. Random Mask Encoding of Multiplexed Phase-Only and Binary Phase-Only Filters. *Opt. Lett.* **1994**, *19*, No. 496.

(38) Liu, V.; Fan, S. S4: A Free Electromagnetic Solver for Layered Periodic Structures. *Comput. Phys. Commun.* **2012**, *183*, 2233–2244.

(39) Peng, Y.; Choi, S.; Kim, J.; Wetzstein, G. Speckle-Free Holography with Partially Coherent Light Sources and Camera-in-the-Loop Calibration. *Sci. Adv.* **2021**, *7*, No. eabg5040.

Recommended by ACS

Light, Matter, Action: Shining Light on Active Matter

Marcel Rey, Giorgio Volpe, *et al.*

APRIL 17, 2023
ACS PHOTONICS

READ 

Neural Operator-Based Surrogate Solver for Free-Form Electromagnetic Inverse Design

Yannick Augenstein, Carsten Rockstuhl, *et al.*

MARCH 29, 2023
ACS PHOTONICS

READ 

Constraining Continuous Topology Optimizations to Discrete Solutions for Photonic Applications

Conner Ballew, Andrei Faraon, *et al.*

JANUARY 09, 2023
ACS PHOTONICS

READ 

Switchable Unidirectional Radiation from Huygens Dipole Formed at an Exceptional Point in Non-Hermitian Plasmonic Systems

Yuto Moritake and Masaya Notomi

FEBRUARY 24, 2023
ACS PHOTONICS

READ 

Get More Suggestions >